

# Structural Changes of PVC Plastisols in Progress of Gelation and Fusion as Investigated with Temperature-Dependent Viscoelasticity, Morphology, and Light Scattering

SEUNG-YEOP KWAK

Division of Polymer Research, Korea Institute of Science and Technology (KIST), P.O. Box 131, Cheongryang, Seoul 130-650, South Korea

## SYNOPSIS

The structural changes of poly(vinyl chloride) (PVC) plastisols during mixing of PVC with a plasticizer was investigated; as the temperature was increased, the system was found to transform from a suspension of solid particles in a liquid medium to a swollen gel and ultimately to a fused homogeneous matrix. The dynamic viscoelastic measurements were utilized to continuously monitor the changes of moduli under a controlled heating rate, employing a mechanical spectrometer. Characteristic changes in the viscoelastic behavior were associated with changes in particulate morphology as observed with a scanning electron microscope (SEM). Both viscoelastic and morphological observations were shown to provide details of structural changes in conjunction with the behavior of the PVC-plasticizer interaction, enabling a qualitative discrimination of the gelation and fusion processes. An *in situ* small-angle light-scattering (SALS) method was performed to make a quantitative estimate for the swollen particles of PVC while they were in the progress of gelation and fusion. From the manner of increase in correlation distances, along with the changes in viscoelastic moduli and morphology, the swelling behavior of the particulate structures were examined on the quantitative basis and brief insight into the complex behavior of the PVC-plasticizer interaction began to be unfolded. © 1995 John Wiley & Sons, Inc.

## INTRODUCTION

Poly(vinyl chloride) (PVC) plastisol is a paste consisting of a mixture of fine particles of PVC resin (dispersion grade) and a plasticizer.<sup>1</sup> The PVC resin is prepared by polymerizing vinyl chloride monomer in the presence of an emulsifying agent (soap) in an aqueous medium, which produces spherical particles (i.e., primary particles) with average size of about 1  $\mu\text{m}$  or smaller in diameter<sup>2</sup> and then by subsequent spray drying and grinding. During the spray drying, the primary particles fuse together and their agglomerates form. The agglomerates are then ground to 15–0.2  $\mu\text{m}$  or smaller,<sup>3</sup> containing various levels of voidage which take up the plasticizer. Within the primary particles, distinct crystalline regions (i.e., microcrystallites) exist, which are acting as cross-

links and are of great importance in preserving the physical strength of PVC.<sup>4,5</sup>

To convert a plastisol into a flexible product, the plastisol is spread on substrates and then heated to a gel and fused.<sup>3</sup> Upon initial heating, PVC particles are swollen with the plasticizer as the plasticizer is absorbed. Simultaneously, the polymer particles become dissolved into the plasticizer from their outer surface, which glues the particles together. At this state, the material is dry but has virtually no mechanical strength. This is called "gelation." Upon further increase in temperature, the swelling and dissolution of more polymer continues and microcrystallites of PVC melt, leading to an eventual uniform mass. This process is called "fusion." Upon cooling, the material develops its rubbery property with an inherent mechanical strength.

Hence, as the gelation and fusion proceed, the retention of the PVC particles, swelling of the particles, and eventual disappearance of the particulate

structure are followed. The objective of the present study was to investigate the manner of the above structural changes in detail from both qualitative and quantitative viewpoints; temperature-dependent viscoelastic measurement, morphology observation, and *in situ* small-angle light-scattering (SALS) were used.

## EXPERIMENTAL

### Plastisol Formulation

A typical commercial PVC resin for the plastisol application was used: Geon 121 (B. F. Goodrich Co.). Its molecular weight is expressed with a relative measure, i.e., inherent viscosity of 1.20 in cyclohexanone at 30°C.<sup>6</sup> Plasticizers used were di-*n*-butyl sebacate (DBS) and diisooctyl phthalate (DIOP).

The plastisol formulation was 60 parts (by weight) of plasticizer per hundred of resin (phr), 3 phr of epoxidized soybean oil, and 2 phr of thermal stabilizer (Ba/Cd/Zn stabilizer). Mixing was done using a mechanical stirrer with a double-blade propeller. The entrapped air was removed by pulling a vacuum on the plastisol. Various characterizations were performed after the plastisols were aged for 2 weeks, during which the viscosity of the plastisol increased rapidly in the beginning and then slowly approached a steady value.<sup>7</sup>

### Viscoelastic Measurement

The Rheometrics mechanical spectrometer (RMS), Model RMS-605, was used in the dynamic oscillatory mode with a controlled heating rate. The 25 mm-diameter parallel-disc assembly was used with a gap set at 2 mm. The frequency of oscillation was maintained at 1 Hz. The temperature of the sample was raised from ambient to 200°C with a programmed increase of 5°C/min. Measurement was taken in a few minutes after reaching the desired temperature in order to attain near-equilibrium values of the viscoelastic properties. The shear strain amplitude was 25% in the range from ambient to 60°C, the onset temperature of gelation. The strain amplitude was then reduced to 2.5%. Those strain amplitudes were not only large enough for an accurate torque signal but also kept in the range of the linear response.

### Morphological Observation

Morphological studies were performed with a scanning electron microscope (SEM), ISI Model SX-40,

at various stages of gelation and fusion. The samples for SEM observation were made by loading a plastisol between plates of RMS and heating up to desired temperatures without imposing shear strain. The sampling temperatures were selected on the basis of characteristic features of the viscoelastic data. The samples were then freeze-fractured at liquid nitrogen temperature and coated with silver to improve the conductivity, and the fracture surfaces were examined.

### Small-angle Light Scattering (SALS)

A time-resolved SALS instrument is schematically shown in Figure 1. A droplet of plastisol was dropped onto a slide glass and covered by a coverglass. This specimen was de-aired by applying vacuum and then mounted on the sample hot stage. The temperature was raised from 40 to 200°C with a programmed heating rate of 2°C/min. The scattered intensity was monitored using the Vidicon camera in conjunction with a detector controller. Then, the analog signal was digitized and analyzed on the Optical Multi-channel Analyzer (OMA) III system. The SALS pattern was scanned in a two-dimensional mode; the scan rate was about 0.5–1.5 s, depending on the number of pixels selected for grouping. Intensities

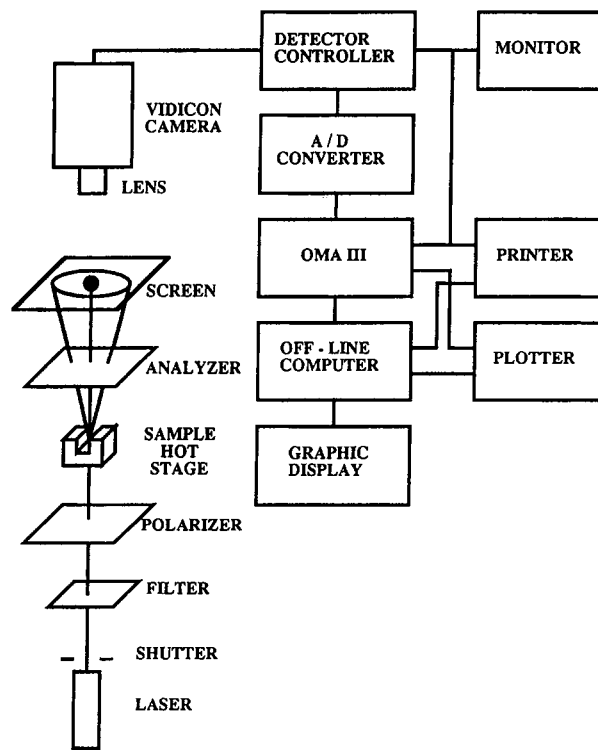
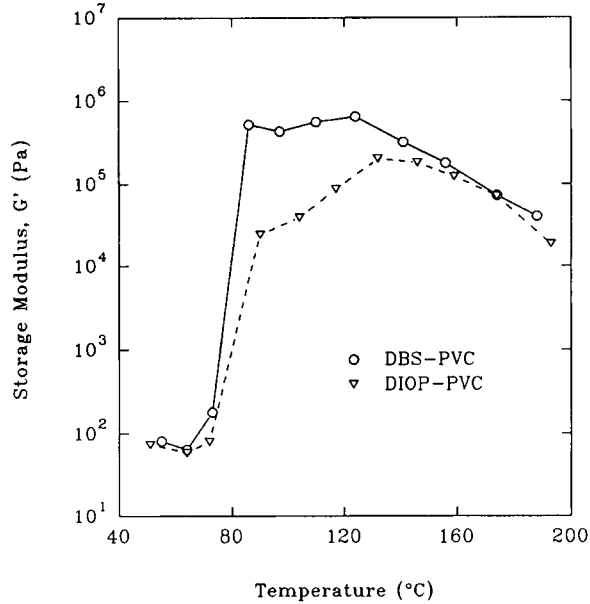


Figure 1 A schematic diagram of the SALS setup.



**Figure 2 (a)** Storage modulus ( $G'$ ) profile of DBS- and DIOP-PVC plastisols during gelation and fusion.

of the scattered light were accumulated as a function of position for each specific temperature.

**RESULTS AND DISCUSSION**

Figure 2(a) and (b) shows the storage modulus,  $G'$ , and loss modulus,  $G''$ , of DBS-PVC and DIOP-PVC

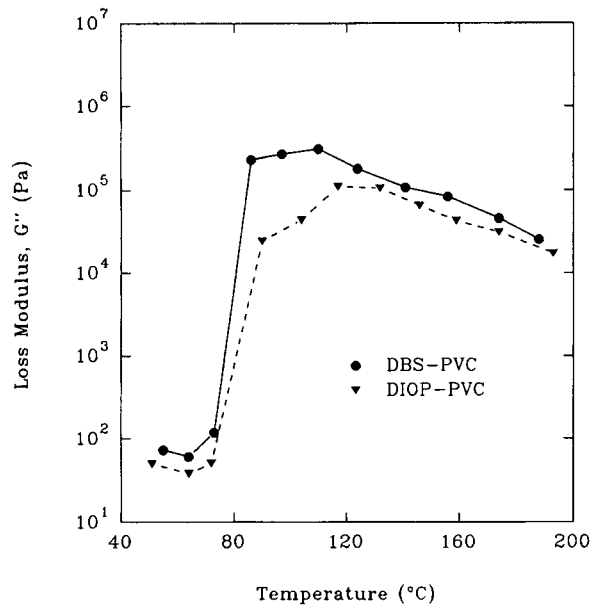


**Figure 2 (b)** Loss modulus ( $G''$ ) profile of DBS- and DIOP-PVC plastisols during gelation and fusion.

plastisols, respectively, being recorded as a function of temperature. In Figure 3, viscoelastic profiles, both  $G'$  and  $G''$ , of the two plastisols are plotted together for a better comparison. As for DBS-PVC plastisol, both  $G'$  and  $G''$  decrease during the initial stage of heating (ca. 55–65°C), implying that the material at this stage remains as a two-phase suspension of PVC particles in the plasticizer. At slightly above 65°C, the gelation process begins and a very steep increase of both moduli by several orders of magnitude occurs between 75 and 85°C; the material has transformed from a liquid paste to a solid, becoming a visually dry mass. A first peak appears in the  $G'$  curve and then the modulus increases slightly, reaching a maximum at about 125°C. The maximum of the modulus corresponds to a completion of gelation and an onset of fusion. With further increase in temperature, both moduli decrease, indicating a dominance of fusion. The decrease of the moduli is due to two processes: First is the normal temperature dependence primarily attributable to the thermal expansion. Second is caused by melting of the PVC microcrystallites which used to act like physical crosslinks in the system.<sup>8</sup>

The overall viscoelastic behavior of DIOP-PVC plastisol is similar to that of DBS-PVC plastisol. However, heating between 75 and 90°C results in an increase of moduli up to slightly above  $10^4$  Pa, by only about two orders of magnitude, and the first peaks as well as the modulus maxima appear at the temperature range 5–10°C higher than that observed

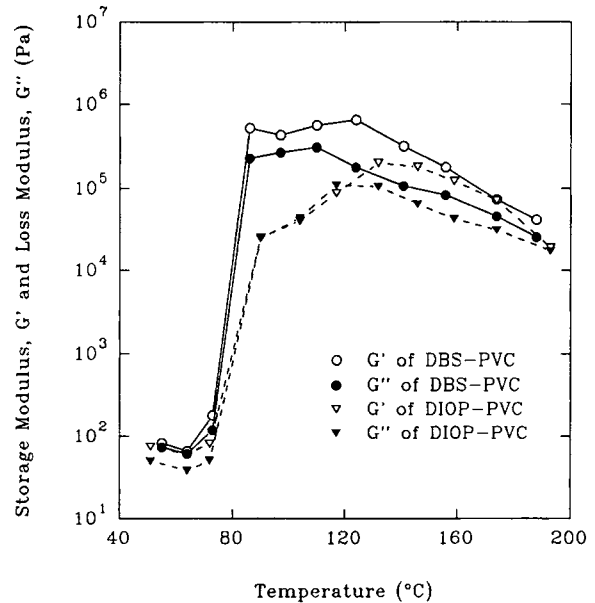


**Figure 3** Viscoelastic profiles (both  $G'$  and  $G''$ ) of DBS- and DIOP-PVC plastisols during gelation and fusion.

with DBS-PVC system; it is apparent that DIOP is, relatively, a poorer solvent than is DBS.

Accompanying changes in morphology were elucidated with SEM for the individual plastisols at various sampling temperatures which were selected with reference to the characteristic features of the viscoelastic curves. The viscoelastic features were the first peak (85°C for DBS-PVC, 90°C for DIOP-PVC),  $G'$  maximum (125°C for DBS-PVC, 135°C for DIOP-PVC), and dominance (160°C for both systems) and end of fusion (185°C for DBS-PVC, 195°C for DIOP-PVC). Figures 4 and 5 are the SEM micrographs of the fracture surfaces of DBS-PVC plastisol at the corresponding temperatures. Figure 4 (top) shows that individual PVC particles are clearly identifiable at 85°C. From this SEM observation and the manner of rapid increase in the dynamic moduli at 75–85°C, as was indicated in Fig-

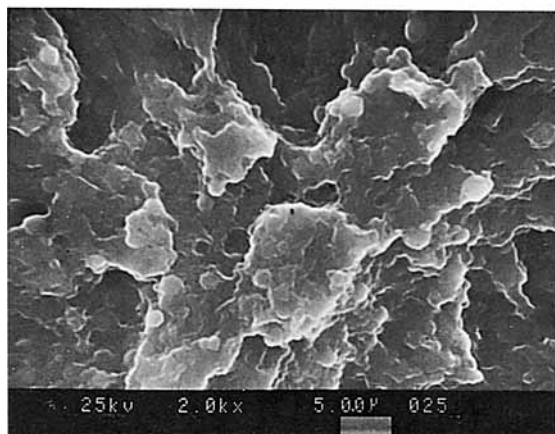
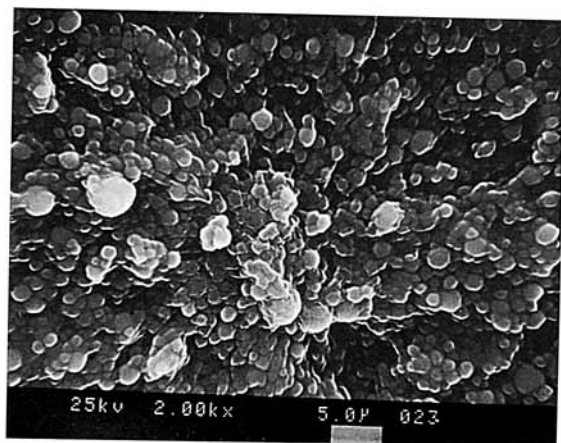


**Figure 4** Scanning electron micrographs of DBS-PVC plastisol (top) at 85°C and (bottom) at 125°C.

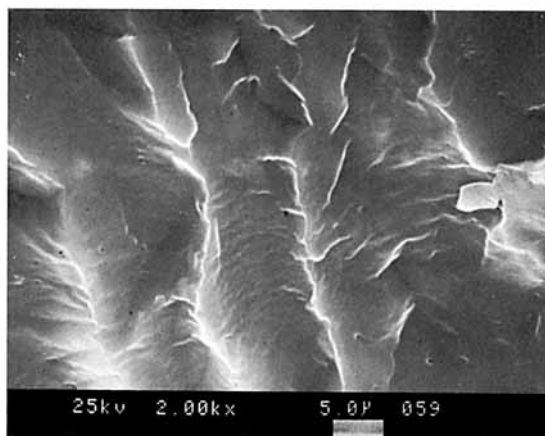
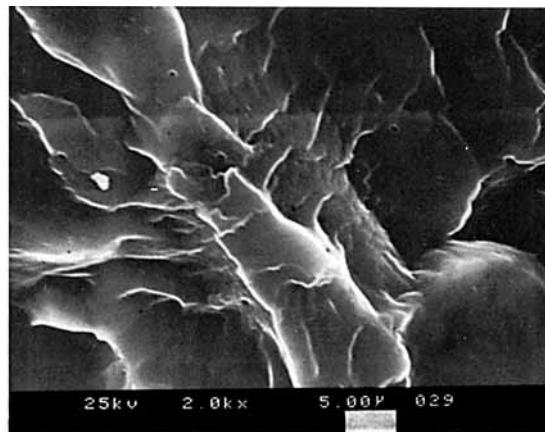


**Figure 5** Scanning electron micrographs of DBS-PVC plastisol (top) at 160°C and (bottom) at 185°C.

ures 2 and 3, it is speculated that the plasticizer penetrates into the voids of agglomerate PVC particles. The particles would have not swollen seriously yet, and this phase makes the response of the system to dynamic deformation to be primarily determined by the particle-to-particle friction, which must contribute to the abrupt increase of moduli.

At 125°C [Fig. 4 (bottom)], which corresponds to the maximum in  $G'$ , structural changes clearly show that only a limited number of original discrete particles are visible and the interparticle boundaries are obscured. It is reasonable to suppose a formation of particle-to-particle junctions across the PVC molecules on the layers of particle surfaces. At 160°C [Fig. 5 (top)], the particulate structure is no longer visible and the particle-to-particle junctions have almost disappeared, which indicates that the particles must have fused to form a uniform plasticized

matrix. At 185°C [Fig. 5 (bottom)], the fracture surface is continuous and the fusion process is believed to be completed.

Next, the morphology of DIOP-PVC plastisol is shown in Figures 6 and 7. Even at 135°C [Fig. 6 (bottom)], the persistence of the particulate structure is still in evidence although the interparticle boundary is diffused. This is contrasted to DBS-PVC at 125°C where a greater portion of PVC particles are considerably swollen and the particulate boundary is more diffused; apparently, DBS possesses a superior solvent power relative to DIOP. In Figure 7 (top), most of particles are shown to have dissolved away from the surface layers of the particles but the memory of some particulate boundaries are more or less recognizable, and, finally, in Figure 7 (bottom), the particles coalesce one another, forming an eventual homogeneous matrix.

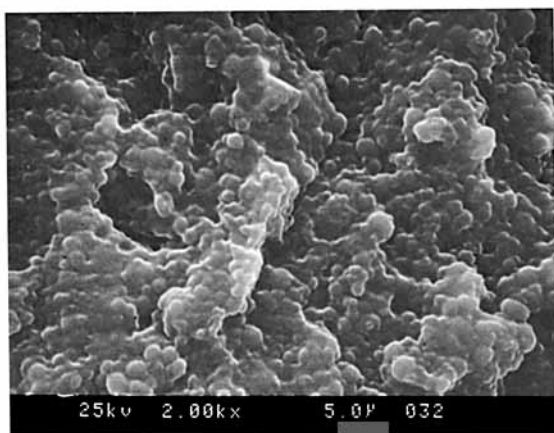
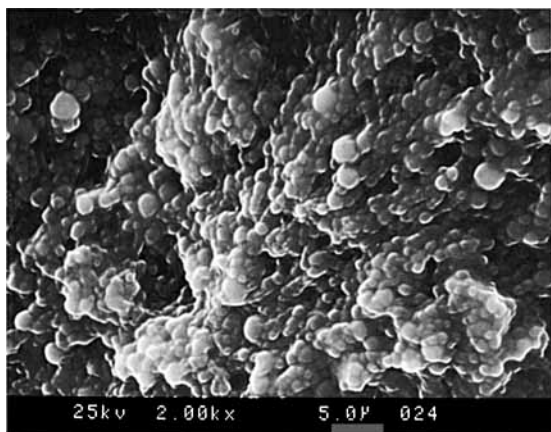


**Figure 6** Scanning electron micrographs of DIOP-PVC plastisol (top) at 90°C and (bottom) at 135°C.

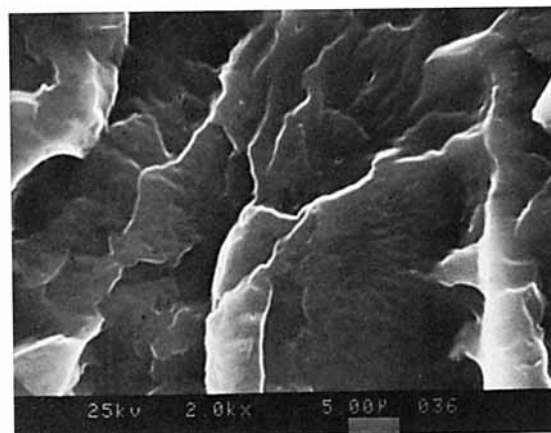
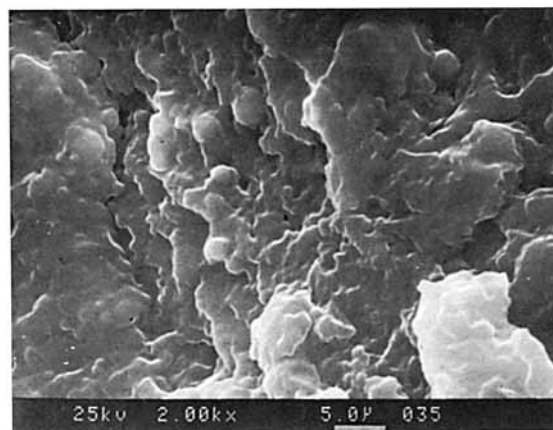


**Figure 7** Scanning electron micrographs of DIOP-PVC plastisol (top) at 160°C and (bottom) at 195°C.

The viscoelastic characterization and SEM provided fingerprints and direct information on the structural changes as the gelation and fusion proceeded; it is noteworthy that the information obtained was qualitative and relative.

An *in situ* SALS method offers a quantitative measure on the structural changes of plastisols followed by the gelation and fusion processes. Figure 8 represents the variations of scattered intensity as a function of the scattering wave number  $q$  at several different temperatures. In this figure,  $q = [4\pi \sin(\theta/2)]/\lambda$ , where  $\theta$  is the scattering angle, and  $\lambda$ , the wavelength of light in the medium. The scattered intensities decay as  $q$  increases, and with increasing temperature, the magnitude of them at  $q < 2$  increases rapidly until reaching a maximum at 146°C and then begins to fall down.

The above observation is illustrated in Figure 9 as the variation of scattered intensity at different

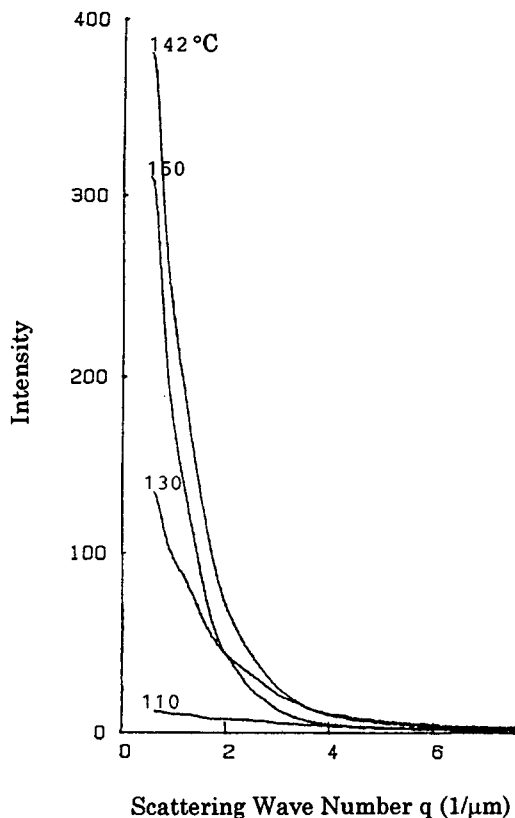


**Figure 8** Scattered intensity vs. scattering wavenumber  $q$  at various temperatures for DIOP-PVC plastisol.

scattering wavenumbers against temperature. The slight increase in the scattered intensity between ca. 70 and 110°C indicates that only a small portion of the PVC particles are swollen by the plasticizer, which is in good agreement with the SEM examination as was shown in Figure 6 (bottom). At this stage, the plasticizer must have been absorbed just inside the pores of the agglomerates. A more significant increase of the scattered intensity above 110°C implies that the plasticizer penetrates into the interior of the PVC particles and makes the particles swollen more seriously, dissolving more polymer, which was also ascertained by the SEM observation in Figures 6 (bottom) and 7 (top). The scattered intensity then reaches a maximum at 146°C and the maximum appears due to the maximum swelling of the particles just before they lose their particle boundaries, corresponding to the completion of gelation.

The DBS-PVC system, although not shown here, indicates an overall scattering behavior similar to that of DIOP-PVC except that the maximum scattered intensity is at 135°C. The temperature difference of about 10°C for the appearance of the inten-

sity maximum in DBS-PVC indicates that DBS fills the available pore volume of the particles earlier than does DIOP. In other words, the gelation process is completed in DBS-PVC earlier than in DIOP-PVC and DBS is apparently a more effective solvent for PVC.

Guinier and Fournet<sup>9</sup> proposed a relationship between the scattered intensity  $I_s$  and the scattering wave number  $q$ , as follows:

$$\ln I_s = \ln(Ka^2) - a^2q^2/4$$

where  $K$  is a constant and  $a$  is a correlation distance. The plot of  $\ln I_s$  against  $q^2$  is called a Guinier plot, illustrated in Figure 10 for DIOP-PVC at 146°C. The value of the correlation distance  $a$  can be obtained from the slope of the straight line drawn by a linear least-square fitting method in the plot:  $a = 2[|\text{slope}|]^{1/2}$ .

The correlation distances  $a$  plotted as a function of temperature for both DIOP-PVC and DBS-PVC plastisols are presented in Figure 11. Although the SALS measurements were performed from 40 to 200°C, it was possible to obtain reliable data between the lower cutoff temperature of 75–100°C and the upper cutoff temperature of 140–150°C. The values of  $a$  for DBS-PVC over the entire temperature range of observation are shown to be larger than those for DIOP-PVC and the largest  $a$  value is for DBS-PVC 1.71  $\mu\text{m}$  at 135°C and for DIOP-PVC 1.35  $\mu\text{m}$  at

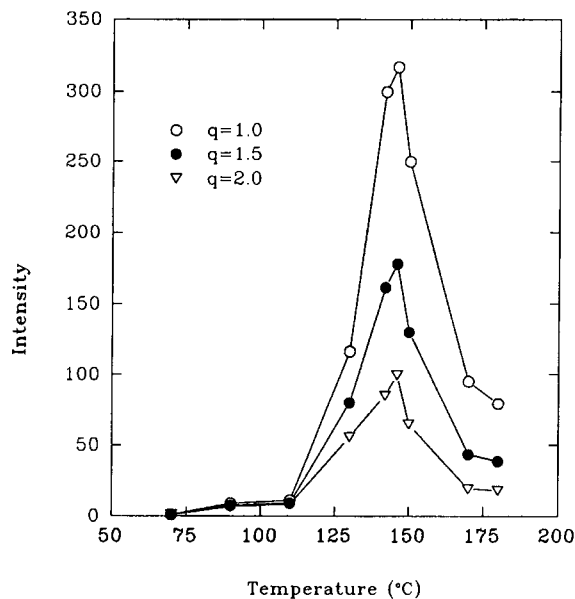


**Figure 9** Scattered intensity vs. temperature at different scattering wavenumber  $q$  for DIOP-PVC plastisol.

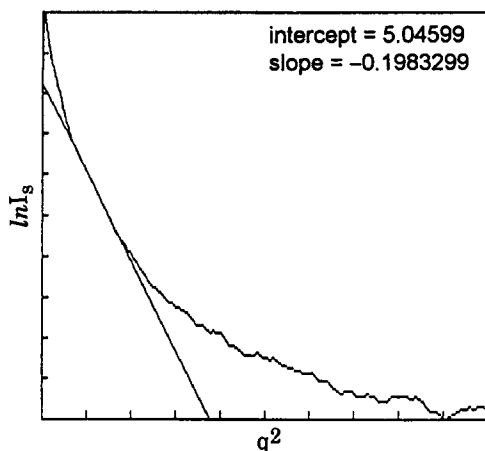


**Figure 10** Guinier plot of DIOP-PVC plastisol at 146°C.

146°C; overall, DBS is proved to be a better solvent as compared to DIOP. Recognizing that the maximum  $a$  value implies the completion of gelation (and as pointed out already, the maximum modulus also corresponds to the completion of gelation), the SALS and viscoelastic methods result in conflicting temperatures for the completion of gelation. Necessarily, the different characterizing methods are responsible for this disagreement. Another possible reason is the different heating rate, i.e., 5°C/min for the viscoelastic method and 2°C/min for the SALS method. However, at present, there is no sufficient observation to answer the above disagreement.

With DIOP-PVC, the slope of increasing  $a$  in Figure 11 is relatively smooth at 100–130°C but becomes steep afterward. On the contrary, DBS-PVC shows a reverse trend; the swelling is more significant at the range of lower temperatures (75–85°C) than at that of higher temperatures. This observation suggests that the temperature dependence of the solvent power is another important consideration for the details of the plasticizer-PVC interaction with the progress of gelation and fusion. In addition, the plasticizer-PVC interaction during gelation and fusion is also time-dependent; a kinetic aspect on the sol-gel transition is required to be sought. These subjects belong to a future publication.

## CONCLUSIONS

In the present article, the complex behavior of the plasticizer-PVC interaction and accompanying structural changes during gelation and fusion of PVC plastisols were systematically unveiled through

a series of characterizations of viscoelasticity, SEM, and SALS.

Interpretation on the viscoelastic moduli developed as a function of temperature and examination of the direct morphology with reference to the viscoelastic properties revealed that the structural changes and eventual homogenization proceeded through the following three stages: The first stage is associated with the decrease of both storage and loss moduli; the PVC particles may have been little affected by the plasticizer, remaining as a two-phase system. The second stage is the rapid increase of the moduli, reaching maxima; the particles become swollen as the plasticizer is taken up and some portion of polymer molecules may have dissolved into the plasticizer from the surface layers of the particles. As the temperature is raised, more swelling and dissolution follow and the amount of glued particles increases, the particle boundaries becoming indiscernible. The third is that the viscoelastic properties decrease with further increase in temperature; the swollen particles eventually coalesce and the inhomogeneity finally disappears.

Quantitative, as well as qualitative, information on the structural changes for PVC plastisols passing through the gelation and fusion processes was obtained by SALS. In particular, calculation of the correlation distances based on the Guinier approximation provided unique, quantitative evaluations on the swelling behavior of the plastisols. From the

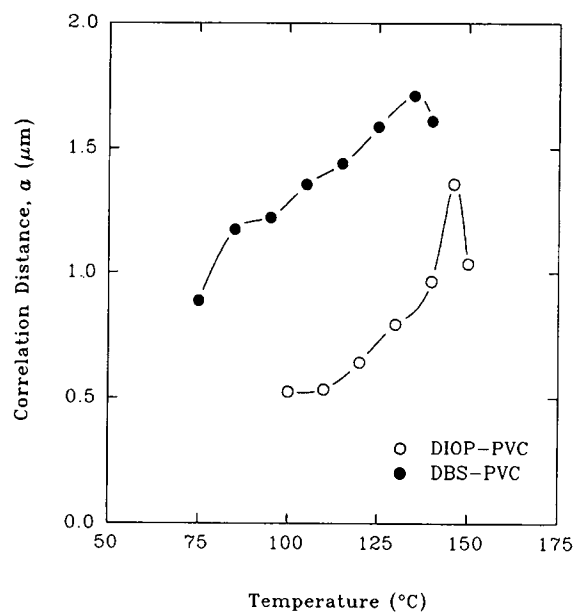


**Figure 11** Correlation distances  $a$  as a function of temperature for DIOP- and DBS-PVC plastisols.

extent of swelling at a given temperature range, together with that of buildup of the viscoelastic moduli, it was possible to relatively contrast the solvent power of individual plasticizers for PVC.

The author wishes to express his appreciation to Dr. N. Nakajima at Institute of Polymer Engineering, The University of Akron, for his valuable discussions and Dr. H. S. Lee at Kolon Industries, Inc., for his assistance in performing the SALS experiments.

## REFERENCES

1. J. A. Davidson and K. Gardner, in *Kirk-Othmer Encyclopedia of Chemical Technology*, M. Grayson and D. Eckroth, Eds., Wiley, New York, 1983, Vol. 23, p. 922.
2. L. I. Nass and C. A. Heiberger, Eds., *Encyclopedia of PVC*, 2nd ed., Marcel Dekker, New York, 1985, Vol. 1.
3. M. L. Berins, Ed., *Plastics Engineering Handbook of the Society of the Plastics Industry, Inc.*, 5th ed., Van Nostrand Reinhold, New York, 1991.
4. H. Munstedt, *J. Macromol. Sci.-Phys.*, **B14**, 195 (1977).
5. J. W. Summers, *J. Vinyl Technol.*, **3**, 107 (1981).
6. C. A. Daniels and E. A. Collins, *J. Macromol. Sci.-Phys.*, **B10**, 287 (1974).
7. N. Nakajima and C. A. Daniels, *J. Appl. Polym. Sci.*, **25**, 2019 (1980).
8. N. Nakajima and S.-Y. Kwak, *J. Vinyl Technol.*, **13**, 212 (1992).
9. A. Guinier and G. Fournet, *Small Angle Scattering of X-rays*, Wiley, New York, 1955.

Received August 29, 1994

Accepted October 7, 1994